◆ Human Brain Mapping 37:2587–2601 (2016) ◆

Structural Connectome Disruption at Baseline Predicts 6-Months Post-Stroke Outcome

Amy Kuceyeski,[1,2]* Babak B. Navi,[2,3] Hooman Kamel,[2,3] Ashish Raj,[1,2] Norman Relkin,[2,3] Joan Toglia,[4,5] Costantino Iadecola,[2,3] and Michael O'Dell[3,4]

[1]*Department of Radiology, Weill Cornell Medical College, New York, New York*
[2]*Feil Family Brain and Mind Research Institute, New York, New York*
[3]*Department of Neurology, Weill Cornell Medical College, New York, New York*
[4]*Rehabilitation Medicine, New York, New York*
[5]*School of Health and Natural Sciences, Mercy College, New York, New York*

Abstract: In this study, models based on quantitative imaging biomarkers of post-stroke structural connectome disruption were used to predict six-month outcomes in various domains. Demographic information and clinical MRIs were collected from 40 ischemic stroke subjects (age: 68.1 ± 13.2 years, 17 female, NIHSS: 6.8 ± 5.6). Diffusion-weighted images were used to create lesion masks, which were uploaded to the Network Modification (NeMo) Tool. The NeMo Tool, using only clinical MRIs, allows estimation of connectome disruption at three levels: whole brain, individual gray matter regions and between pairs of gray matter regions. Partial Least Squares Regression models were constructed for each level of connectome disruption and for each of the three six-month outcomes: applied cognitive, basic mobility and daily activity. Models based on lesion volume were created for comparison. Cross-validation, bootstrapping and multiple comparisons corrections were implemented to minimize overfitting and Type I errors. The regional disconnection model best predicted applied cognitive ($R^2 = 0.56$) and basic mobility outcomes ($R^2 = 0.70$), while the pairwise disconnection model best predicted the daily activity measure ($R^2 = 0.72$). These results demonstrate that models based on connectome disruption metrics were more accurate than ones based on lesion volume and that increasing anatomical specificity of disconnection metrics does not always increase model accuracy, likely due to statistical adjustments for concomitant increases in data dimensionality. This work establishes that the NeMo Tool's measures of baseline connectome disruption, acquired using only routinely collected MRI scans, can predict 6-month post-stroke outcomes in various functional domains including cognition, motor function and daily activities. *Hum Brain Mapp 37:2587–2601, 2016.* © 2016 Wiley Periodicals, Inc.

Key words: connectome; imaging biomarkers; statistical modeling; outcome assessment; stroke; magnetic resonance imaging

Additional Supporting Information may be found in the online version of this article.

Contract grant sponsors: Leon Levy Foundation Fellowship (to A.K.), the Peter Jay Sharp Foundation (to M.O.), the Florence Gould Endowment for Discovery in Stroke (to B.N.); Contract grant numbers: NIH; K23-NS091395 (to B.N.), NS-34179 (to C.I.), K23-NS082367 (to H.K.), P41-RR023953-02 (to A.R.), P41-RR023953-02S1 (to A.R.), and R01-NS075425 (to A.R.)

*Correspondence to: Amy Kuceyeski, Weill Cornell Medical College, 407 East 61st Street, R-115 New York, New York 10065. E-mail: amk2012@med.cornell.edu

Received for publication 23 November 2015; Revised 17 February 2016; Accepted 14 March 2016.

DOI: 10.1002/hbm.23198

Published online 26 March 2016 in Wiley Online Library (wileyonlinelibrary.com).

INTRODUCTION

Stroke affects approximately 800,000 people in the U.S. each year and is a major cause of adult disability [Mozaffarian et al., 2014]. Impairments after stroke often include motor and language dysfunction, but there can also be more subtle cognitive and general impairments that directly affect a patient's quality of life. Accurate clinical prognoses are critical for policy makers and physicians to develop effective rehabilitation plans and for patients and their caregivers to plan for the future. Imaging biomarkers, in particular those of the structural connectome, have increasingly played an important role in predictions of chronic post-stroke outcomes [Auriat et al., 2015; Crofts et al., 2011; Imura et al., 2015; Johansen-Berg et al., 2010; Mukherjee, 2005; Venkatasubramanian et al., 2013], see Grefkes and Fink, [2014] for a review. The connectome, or map of structural and functional connections in the brain, has become commonplace in the neuroscience literature, starting with work by Sporns et al. [2005]. Since then, a wealth of studies investigating the relationship between connectome structure and ability in healthy subjects[Li et al., 2009; Wen et al., 2011], as well as connectome disorder/disruption and disability in subjects with various psychiatric and neurological disorders have been published [Belmonte et al., 2004; Skudlarski et al., 2010; Stam et al., 2007; Supekar et al., 2008]. In particular, measures of both local and remote white matter connectome disruption in stroke have been shown to predict motor [Puig et al., 2013], language [Hope et al., 2013] and cognitive recovery [Warren et al., 2014]. However, few quantitative imaging-based studies have focused on broader measures of activities that are likely related to distributed networks within the brain and that affect quality of life, such as general cognition, basic mobility, and daily activities [Cheng et al., 2014; Imura et al., 2015].

The Network Modification (NeMo) Tool [Kuceyeski et al., 2013] quantifies disruptions in the brain's structural network by mapping areas of damage or abnormality onto a large collection of healthy connectomes. It is one of a limited, albeit increasing, number of studies that have utilized healthy connectome information to predict network effects in various pathological states [Boes et al., 2015; Honey and Sporns, 2008; Raj et al., 2012; Seeley et al., 2009]. The NeMo Tool has recently been used to investigate lesion-dysfunction relationships [Kuceyeski et al., 2015b] and longitudinal remote degeneration [Kuceyeski et al., 2014] in stroke. It has also been used to relate white matter and gray matter pathologies in normal aging [Glodzik et al., 2014] and reveal lesion-symptom relationships in subtle cognitive impairment associated with early multiple sclerosis [Kuceyeski et al., 2015a]. Two main advantages of the NeMo Tool are that it uses MRI sequences routinely obtained in the acute clinical setting and does not require expertise in advanced diffusion image processing and tractography. This allows for a clinically feasible method of quantitatively estimating from an MRI in the acute phase of stroke the pattern of disconnection with the aim of providing insight into post-stroke outcomes. The NeMo Tool allows estimation of connectome changes at three different levels: changes in whole brain network metrics (global), changes in the connectivity of gray matter regions to the rest of the network (regional) and changes in connectivity between pairs of gray matter regions (pairwise). In network terms, the regional level measure is akin to changes in a node's degree while the pair-wise level measure is akin to changes in edge strength. In this work, we hypothesized that models based on the NeMo Tool's measure of baseline regional and pairwise connectome disruption would better predict 6-month post-stroke functional outcomes than models based on lesion volume measures or global connectome disruption measures, which is most similar to what is used clinically.

Abbreviations

AMPAC	Activity Measure for Post Acute Care
CST	Cortico-spinal tract
DWI	Diffusion-weighted images
FA	Fractional anisotropy
MNI	Montreal Neurological Institute
NYP	New York-Presbyterian

METHODS

Subjects and Data

One hundred and twenty-one patients with acute stroke were admitted to the inpatient rehabilitation unit at New York-Presbyterian (NYP) Hospital/Weill Cornell Medical Center between July 2012 and February 2015 and provided consent for participation in this IRB-approved study. Subjects were included if they had (1) ischemic stroke, (2) MRI scans acquired at NYP within 14 days of stroke, (3) apparent hyper-intensities on diffusion-weighted images (DWI) and (4) completed 6-month follow-up testing. One subject was excluded due to a concurrent cancer diagnosis whose treatment would influence their rehabilitation and recovery after stroke. Forty subjects (age: 68.1 ± 13.2 years, 17 female, NIHSS: 6.8 ± 5.6) satisfied these inclusion criteria (see Supporting Information Table I for cohort characteristics). T1 and DWI sequences were collected within 14 days of stroke on 1.5 Tesla (24 subjects) or 3.0 Tesla (16 subjects) GE Signa EXCITE scanners (GE Healthcare, Waukesha, WI). The DWI sequences (on both 1.5 T and 3.0 T) were acquired axially via an echo-planar imaging sequence, with $b = 1{,}000$ s/mm^2 and $b = 0$ s/mm^2 from 30 5-mm thick slices and 128×128 matrix size, 1 mm in-plane resolution, 240 mm FOV, and repetition time/echo time/inversion time = 8,000, 9,000 or 10,000/70-100/0 ms. T1 scans were acquired axially (repetition time/echo time/inversion time- = 500/10/0 ms for 1.5 T and 1,700/7 or 21/725 for 3.0 T)

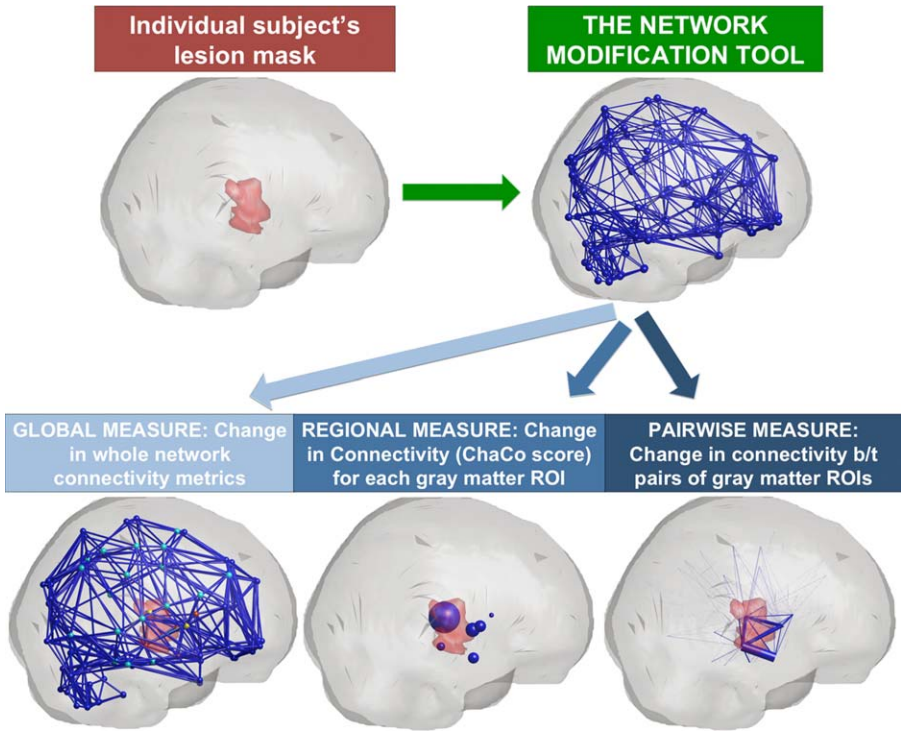

Figure 1.
A schematic of the Network Modification Tool and how it is used to estimate the three levels of structural connectome disruption (global, regional and pairwise) due to a given individual's stroke lesion. [Color figure can be viewed in the online issue, which is available at wileyonlinelibrary.com.]

with a 256 × 256 matrix over 30 5.0-mm thick slices with 0.5 mm in-plane resolution and 240 mm FOV.

Our functional outcome measure was the computer-adaptive version of the Activity Measure for Post Acute Care (AMPAC^{TM}), which was performed on subjects upon discharge from the rehabilitation facility and again at 6 months post-stroke via telephone. The AMPAC was designed to assess post-acute functionality in adults and assesses three domains: (1) applied cognitive functioning (e.g., using a phone, following complex instructions, reading print material), (2) basic mobility (e.g., ambulation, transfers, lifting, bending, lifting, carrying) and (3) daily activities (e.g., feeding, grooming, dressing, meal preparation) [Haley et al., 2004]. Patients assign a level of difficulty (no difficulty, a little difficulty, a lot of difficulty, cannot/unable to do) to each of the functional tasks and activities in the AMPAC. The AMPAC was implemented due to the minimal time required, ease of use and the fact that it could be administered over the phone. This test has been validated in post-acute care patients with major neurological, orthopedic, and medical conditions [Andres et al., 2004; Jette et al., 2007; Siebens et al., 2005]. Scores are between 0 and 100 where high scores indicate less difficulty and need for assistance.

Image Processing and the NeMo Tool

Lesion masks in this cohort were created and processed as in our previous studies [Kuceyeski et al., 2014; Kuceyeski et al., 2015b]. Specifically, masks indicating acute stroke injury as identified by apparent DWI hyperintensities were hand drawn by two raters (BN and AK) using FSLview [Smith et al., 2004]. Inter-rater agreement of the lesion masks was assessed using Dice's similarity index [Dice, 1945], a measure which is widely used to assess voxel-wise agreement of binary lesion masks [Zou et al., 2004]. A Dice's index of between 0.6 and 0.8 is considered good [Seghier et al., 2008]. The stroke subjects' T1 scans were normalized to Montreal Neurological Institute (MNI) space using linear followed by non-linear normalization in SPM8 [Friston et al., 2006], and these transformations were then applied to the DWI mask with nearest neighbor interpolation.

The NeMo Tool estimates structural connectome disruption that arises from a given lesion mask or area of pathology. It does so by superimposing the patient's lesion mask on a database of normal control connectomes that have been coregistered to a common space (Montreal Neurological Institute, or MNI space) (see Fig. 1). Seventy-three healthy subjects (40 men, 33 women, 30.2 ± 6.7 years) were used to create the normal connectomes, see Kuceyeski

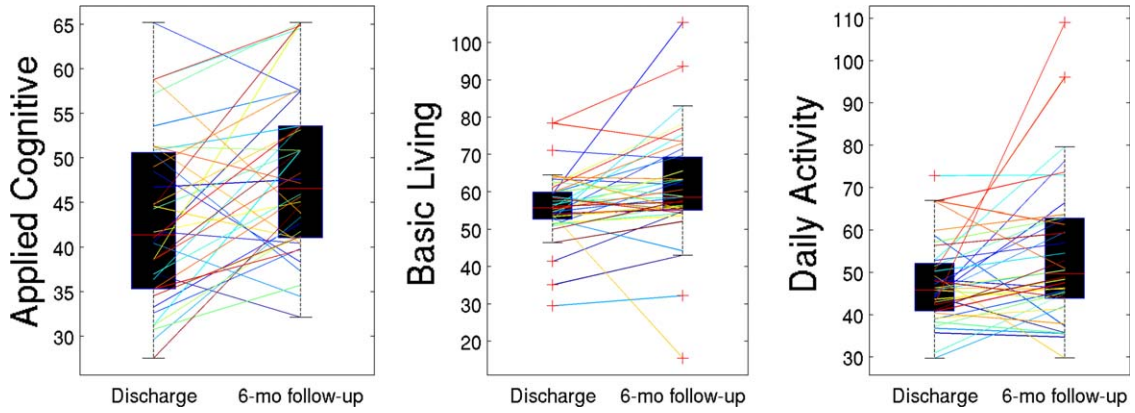

Figure 2.

Change in each of the AMPAC scores from discharge to 6-months follow-up: boxplots represent the distributions over all subjects while lines represent each individual. [Color figure can be viewed in the online issue, which is available at wileyonlinelibrary.com.]

et al., [2013] for details. Briefly, diffusion MRIs (55-direction HARDI acquired, $b = 1000$) were corrected for eddy current and motion artifacts using FSL [Smith et al., 2004] and T1 images were segmented and parcellated into 116 gray matter regions in the AAL atlas [Tzourio-Mazoyer et al., 2002]. The orientation distribution function of the pre-processed diffusion data was reconstructed using a spherical harmonic representation of q-ball imaging [Hess et al., 2006]. The surface voxels of the parcellated cortical and subcortical structures were used to seed the probabilistic tractography algorithm. The tractography algorithm used incorporated tissue classification probability and orientation distribution information in a Bayesian manner, allowing for crossing and kissing fibers [Iturria-Medina et al., 2005]. In this work, we averaged the nine regions in the left cerebellum, nine in the right cerebellum and eight regions in the vermis in the 116-region AAL atlas to yield a total of 93 ROIs in the final connectome. Global network metrics, such as efficiency and characteristic path length, were calculated on the weighted network that was constructed by counting the total number of fibers between pairs of regions. Each individual's network was then normalized by their total fiber count (sum of the network edges) to control for head size variations across the population. The NeMo Tool estimated structural connectome disruption for each patient's lesion mask at three different levels: (1) the global, whole-brain level, (2) at the level of individual gray matter regions and (3) at the level of connections between pairs of gray matter regions. Global connectome disruption is estimated by removing streamlines that pass through the lesion mask and recalculating the "lesioned" whole brain tract count network and resulting network metrics. We normalized the "lesioned" tract count network by the total fiber count in the original (intact) network since normalizing by the number of new (smaller) fibers would cause network edges that were not damaged to increase compared to their original values, which is not physiological or interpretable. Regional connectome disruption is estimated via the Change in Connectivity (ChaCo) score [Kuceyeski et al., 2013]. The ChaCo score corresponds to the percent of streamlines connecting to a given gray matter region that pass through an area of infarct. In this analysis, higher ChaCo scores corresponded to a higher percent of estimated connectivity disruption experienced by a given region as a result of the infarct. Pairwise connectome disruptions are quantified by taking the z-score of the pairwise connections, or edges in the connectivity network, in the "lesioned" network compared to the normal connectomes in the NeMo Tool. Global, regional and pairwise scores were calculated using each of the 73 normal controls' tractograms and the mean over these scores taken to be the final value. Finally, for comparison, we also constructed a model based on lesion volume (log transformed).

Predicting Six-Month APMAC Scores: Global, Regional and Pairwise Level Models

Four different models predicting six-month AMPAC scores were compared, based on (1) lesion volume, (2) global connectome disruption measures, (3) regional connectome disruption measures (ChaCo scores) and (4) pairwise connection disruption measures. The modeling approach used here is similar to the work done in our previous paper that predicted baseline functional and impairment scores [Kuceyeski et al., 2015b]. Specifically, Partial Least Squares Regression (PLSR) models at each of the three levels were constructed for each of the three follow-up (6 month) AMPAC scores. Non-imaging input variables in each of the models included age, gender, years of education, previous cerebrovascular accident (CVA), length of stay in the rehabilitation facility, months of therapy after discharge and discharge AMPAC score. Input variables of connectome disruption estimated via the NeMo tool

TABLE I. Summary of the raw AMPAC scores as well as the model diagnostics for the models based on lesion volume, global, regional and region-pair disconnection

	Raw scores			Lesion volume			Global model			Regional model			Pairwise model		
AMPAC subtest	Dis-charge	Follow-up	*t*-statistic (*p*-value[a])	R^2	Δ_i w_i	# Comp	R^2	Δ_i w_i	# Comp	R^2	Δ_i w_i	# Comp	R^2	Δ_i w_i	# Comp
Applied cognitive	42.9 ± 9.4	48.2 ± 9.1	−2.62 (0.037)	0.37	7.3 2.3%	2	0.38	8.7 1.1%	2	0.56	0 85.6%	2	0.45	4.1 11.0%	2
Basic mobility	56.1 ± 9.0	61.2 ± 15.1	−2.53 (0.045)	0.55	3.8 10.7%	2	0.53	5.8 3.9%	2	0.70	0 71.0%	3	0.62	3.2 14.3%	3
Daily activity	47.4 ± 9.8	54.0 ± 16.6	−3.52 (0.0033)	0.40	8.6 1.2%	2	0.41	8.4 1.3%	2	0.62	3.9 12.2%	4	0.72	0 86.6%	4

[a]Bonferroni corrected for three multiple comparisons.
Shaded cells within the body of the table indicate the models with the best model fit/lowest AIC values for each of the three AMPAC scores.

depended on the model's level. The lesion volume model included one imaging-based metric: logarithm of lesion volume. The global level model included two imaging-based measures per subject: efficiency and characteristic path length. The regional level model initially included 93 imaging-based measures per subject, i.e., the ChaCo scores for each of the 93 gray matter regions considered. The pairwise level model initially included 661 pairwise connections [out of $(93 \times 92)/2 = 4278$ possible] that were present in all of the 73 normal connectomes in the NeMo Tool. There may be some variations in the presence of edges across individuals due to population variability, noise present in imaging and post-processing, etc. In order to focus on region-pairs that have the highest probability of connection, we investigated those edges that existed in all 73 normal controls. In addition, due to population heterogeneity of lesion location, we chose to include only those regions or region-pairs that had non-zero disconnection in at least 10 subjects (25% of the total population). This procedure further minimized the possible influence of measures with low signal in the sample. After removing those measures with low signal, we were left with ChaCo scores from 91/93 gray matter regions and disconnection scores from 490/661 pairwise connections. We investigated the influence of varying the number of subjects used for the low signal cutoff in the model results (which were largely minimal, see Supporting Information Methods II).

PLSR is advantageous in situations where there exist many more input variables than available data points, as the data gets reduced to a parsimonious set of statistically relevant components. PLSR reduces the dimensionality of the input variables by combining them into new variables (components) that have maximum correlation with the outcome variable, followed by regression on the new

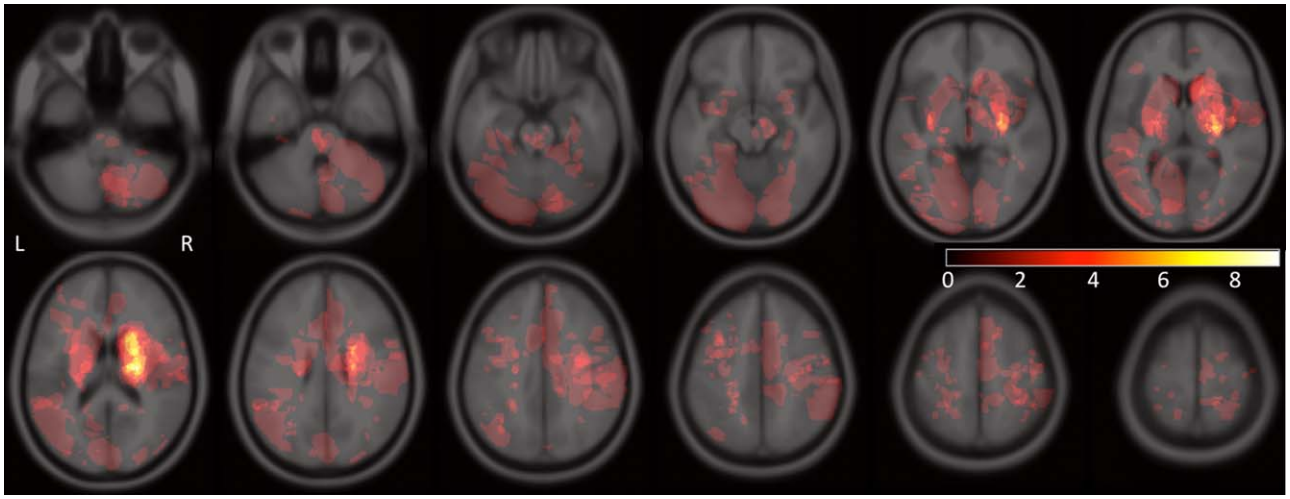

Figure 3.
A heat map of the lesion areas for all 40 subjects included in the study. Color indicates the number of subjects that have the particular voxel included in their lesion masks (colorbar: no color = 0, white = 9).

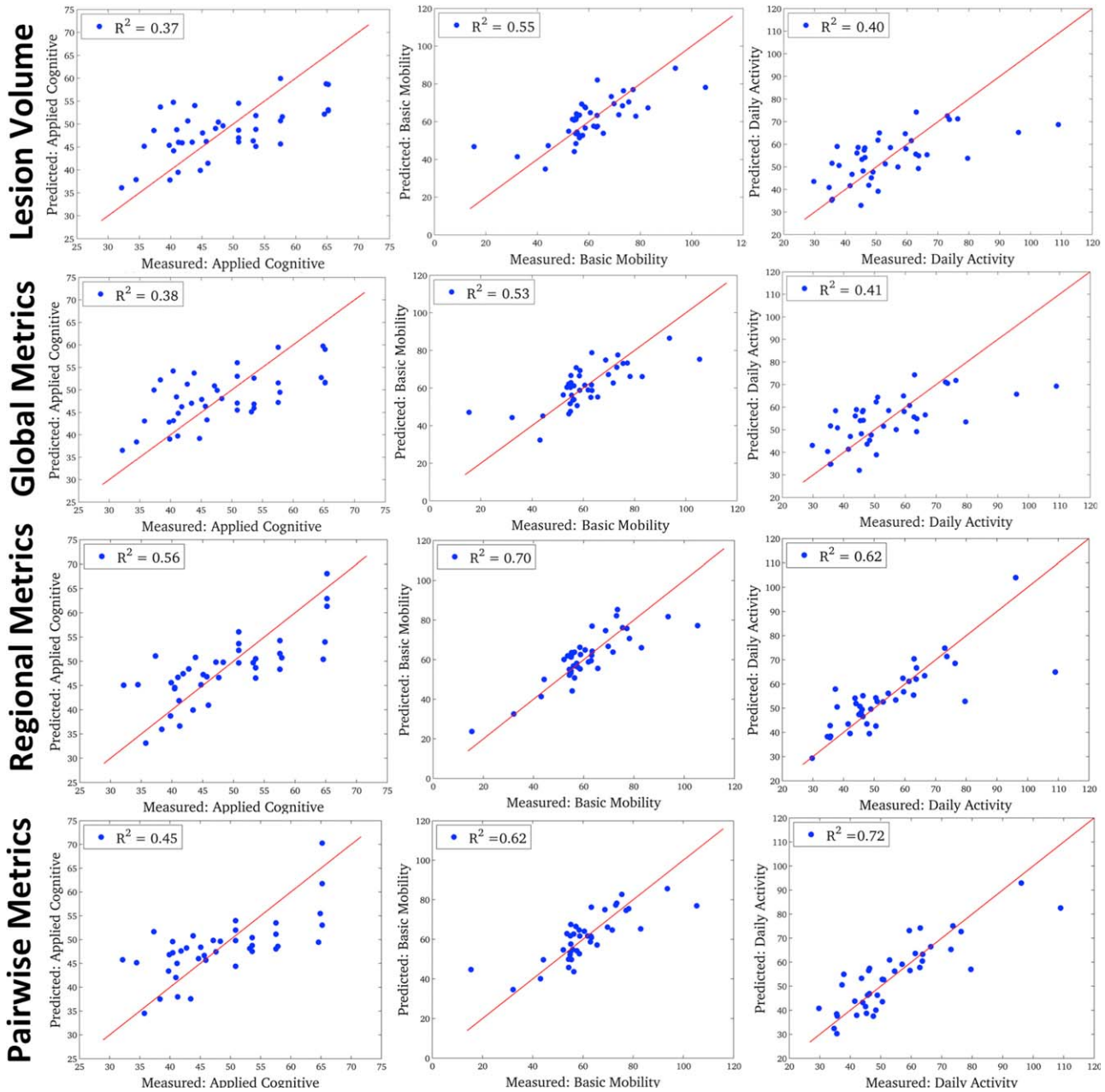

Figure 4.

The predicted versus true AMPAC scores for the four levels of fixed-effects PLSR models: lesion volume model (top row), global model (second row), regional level (third row) and pairwise level (bottom row). The three AMPAC subscores are arranged in columns: applied cognitive (left column), basic mobility (middle column) and daily activity (right column). [Color figure can be viewed in the online issue, which is available at wileyonlinelibrary.com.]

variables. Each newly created component is independent of the others, making PLSR advantageous when input variables may be co-linear. The final number of components for the final model were chosen via jackknife cross-validation to minimize data over-fitting, and the stability of the model was assessed by bootstrapping 30,000 samples with replacement [Krishnan et al., 2011]. Confidence intervals (CIs) for the regression coefficients were calculated using the bias-corrected and accelerated percentile method [Efron, 1987]. CIs were corrected for multiple

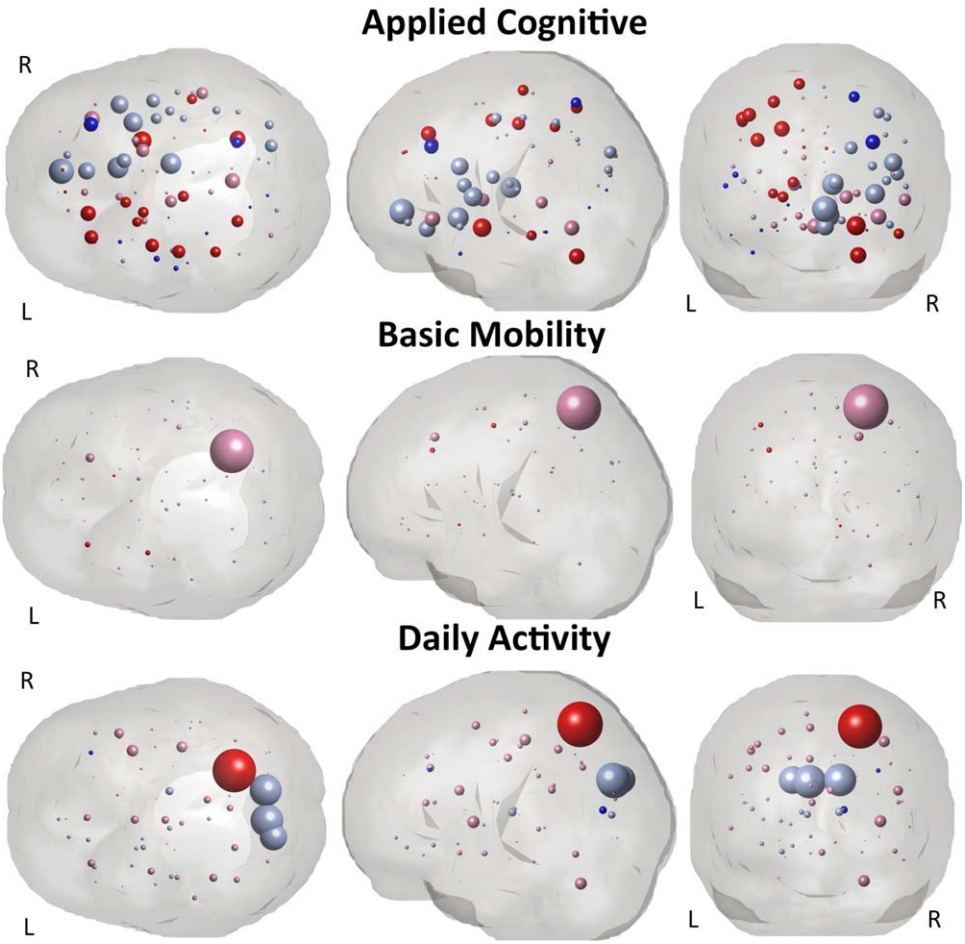

Figure 5.

Visualization of the PLSR regression coefficients for the regional model that had disconnection measures for each gray matter region (ChaCo scores) as input variables. Spheres represent each of the 93 gray matter atlas regions. The radius of the sphere is proportional to the size of the median of the PLSR coefficient (over the bootstrapped samples) while color denotes significance and directionality: bright red and pale red indicate negative coefficients (more disconnection = worse f/u) and bright blue and pale blue indicate positive coefficients (more disconnection = better f/u). Bright colors denote significant coefficients while the pale colors denote non-significant coefficients. The three AMPAC subscores are arranged in rows: applied cognitive (top row), basic mobility (middle row) and daily activity (bottom row). Note: The scale of the spheres is identical for the basic mobility and daily activity while the applied cognitive is twice the scale of the others (for visualization purposes).

comparisons over the three PLSR models for each AMPAC score and the various amount of input variables within each level using the Sidak method [Šidák, 1967]. If the multiple comparisons adjusted CI for a particular input variable did not include zero, it was considered a significant predictor for that assessment (see Supporting Information for details). PLSR coefficients for the brain regions and region-pairs were illustrated via glassbrains created using Brainography, a visualization software developed within our lab [LoCastro et al., 2014]. Overall performance was compared for the three model levels via R^2 values, which measure goodness-of-fit, and Akaike Information Criterion (AIC) [Burnham and Anderson, 2002], which measure goodness-of-fit while considering model complexity. The difference in AIC for model i from the minimum AIC across all models ($\Delta_i = AIC_i - \}min\, AIC$) provides a way to relatively compare models that have different input variables. In general, $\Delta_i < 2$ indicates substantial evidence for the model, $2 < \Delta_i < 7$ indicate less support while $\Delta_i > 10$ indicates that the model is quite unlikely. Finally, we calculated the Akaike weights of each of the M models considered, i.e., $w_i = \exp(-\Delta_i/2)/\sum_M \exp(-\Delta_i/2)$. The Akaike weights provide the probability that the model is the best among all candidate models [Burnham and Anderson, 2002]. All models and statistical tests were performed using relevant programs within Matlab.

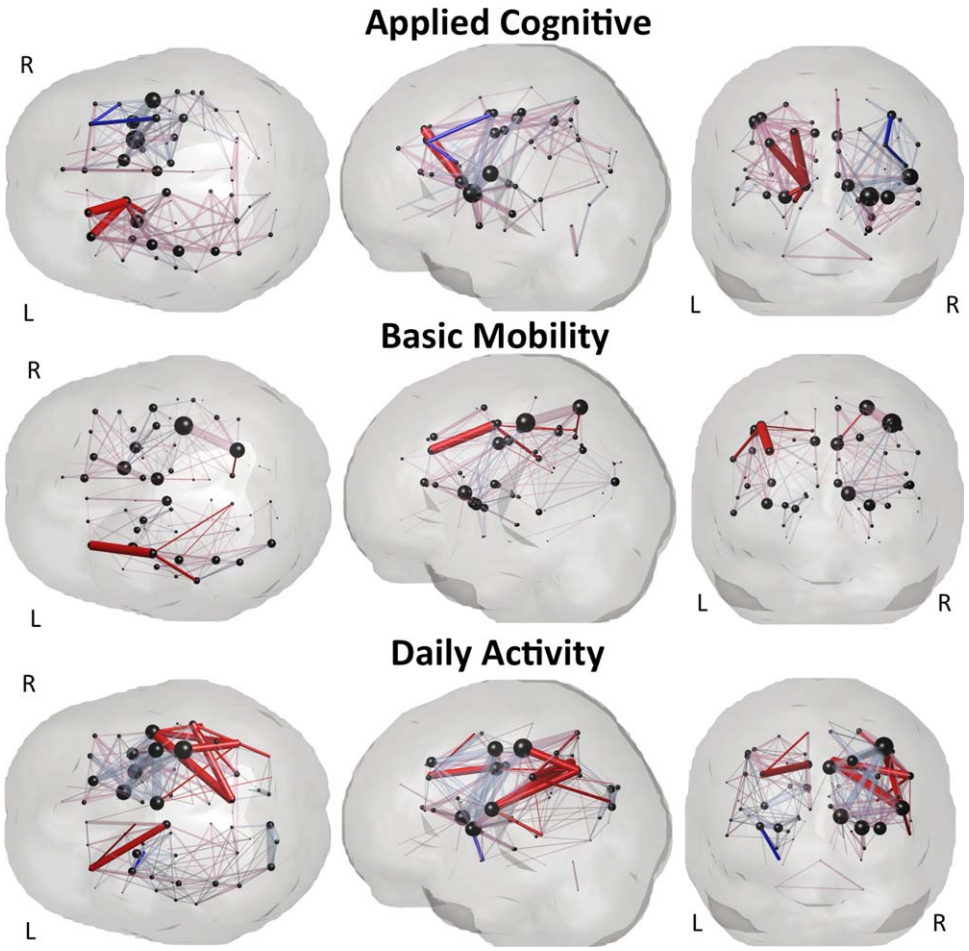

Figure 6.

Visualization of the PLSR regression coefficients for the pairwise model that had disruptions of white matter connections between pairs of gray matter regions as input variables. Spheres represent the 93 gray matter regions while pipes between them represent the regression coefficients for the pairwise disconnection between the two gray matter regions. Pipe size is proportional to the value of the median of the PLSR coefficient (over the bootstrapped samples), while color denotes significance and directionality: bright red and pale red indicate negative coefficients (more disconnection = worse f/u) and bright blue and pale blue indicate positive coefficients (more disconnection = better f/u). Bright colors denote significant coefficients while the pale colors denote non-significant coefficients. The size of the spheres is proportional to the outgoing degree in the coefficient network—the larger the sphere the larger the sum of the magnitude of the pairwise coefficients involving that gray matter region. Note: the pipes do NOT represent the spatial location or geometry of the white matter fibers connecting the two gray matter regions, they are drawn as straight lines between the spheres.

RESULTS

The subjects in general had increases in their AMPAC scores from baseline to 6-months follow-up: paired *t*-tests showed significant increases (after Bonferroni correction for three multiple comparisons) from baseline to follow-up in each of the subscores (see Table I). Figure 2 shows the AMPAC scores from discharge to 6-month follow-up over the population as a whole via a boxplot and while each individual is represented as a different line. The minimal detectable change (MDC) is the smallest change that can be detected by a scale that corresponds to a noticeable change in ability. The change in the mean Applied Cognitive scores is just below the established MDC of 5.55, while the other scores have change in means that are above the established MDC (Basic Mobility: MDC = 4.28; Daily Activity: MDC = 3.70) [Jette et al., 2007].

A heatmap of the lesion masks, coregistered to MNI space is given in Figure 3. Dice's similarity index of inter-rater agreement between two raters for the lesion mask creation was 0.77 ± 0.13 (IQR: 0.70-0.85), which is at the high end of the good range [McHugh, 2012; Seghier et al., 2008].

To further investigate the influence of noise at the level of the lesion masks, we correlated the ChaCo scores and pairwise disconnection measures of the two rater's lesion masks. The Spearman's correlations were 0.97 and 0.95 for the ChaCo scores and pairwise disconnection scores, respectively (see Supporting Information Fig. I). We conclude that noise present at the level of lesion masks has minimal impact on the final disconnection scores. We also investigated the effect of varying the "low-signal" threshold, i.e., the number of subjects in which a disconnection score had to be present to be included in the regional and pairwise models. The model statistics (R^2 and AIC) were almost identical for each threshold applied in both the regional and pairwise level models. In the region-level model, the significant variables were largely unchanged while in the pairwise-level model, the significant coefficients of smaller magnitude, which were mostly positive, became non-significant as the threshold increased (see Supporting Information Methods II).

The regional models had the best goodness-of-fit and lowest AIC for both the basic mobility and applied cognitive subscores while the pairwise model had the best goodness-of-fit and lowest AIC values for the daily activity subscore (see Table I). The difference in AIC values between the best model and the others are generally between 3 and 7, indicating there is less evidence for the other models. The relative probabilities (Akaike weights) for the best models, all over 70%, confirm this finding. The model statistics in Table I also show that the lesion volume/global models perform worse than the regional/pairwise models: they explain 15-30% percent less variance, have a difference in Akaike scores of more than 3 and have much lower probability. In fact, the highest probability (Akaike weights) of all six of the lesion volume/global measure models is only 10%. Figure 4 shows the predicted versus true AMPAC subscores for the four fixed-effects model levels: lesion volume (top row), global (second row), regional (third row) and pairwise (bottom row).

Inspection of confidence intervals of the PLSR coefficients enabled identification of input variables that were significant predictors of a given outcome measure. Supporting Information Tables II, III and IV list the significant PLSR coefficients and their median values over the bootstrapped samples for the lesion volume, global, regional and pairwise level models, respectively. Shading in those tables indicates non-imaging demographic variables. The PLSR coefficients for each of the gray matter structures in the regional level models are visualized in Figure 5, where each sphere represents a particular gray matter region. Sphere size is proportional to the relative size of the median PLSR coefficient (over the bootstrapped samples), while color indicates significance and directionality: bright blue (significant positive influence), pale blue (non-significant positive influence), bright red (significant negative influence) or pale red (non-significant negative influence). Positive influence means that more disconnection is related to better follow-up while negative coefficients mean more disconnection is related to worse follow-up. The PLSR coefficients for the pairwise model are visualized in Figure 6, where the pairwise connections are represented as pipes drawn in a straight line connecting the two relevant gray matter regions, which are again represented by spheres. Pipe thickness is proportional to the value of the coefficient while color denotes the same directionality and significance as in Figure 5. The size of the spheres is proportional to the outgoing degree in the coefficient network—the larger the sphere the larger the sum of the magnitude of the pairwise coefficients involving that gray matter region.

DISCUSSION

In this work, we successfully applied the NeMo Tool's measures of baseline connectome disruption to predict long-term post-stroke recovery using routinely collected MRI scans. A similar approach was previously used to predict baseline dysfunction in the acute stages after stroke [Kuceyeski et al., 2015b]. Here, we extended the approach to incorporate details about post-stroke therapy and other patient demographics to predict long-term recovery. In addition, we compared models at varying levels of connectome disruption, such as whole brain, gray matter regions and gray matter region pairs, to determine the best level at which to predict various long-term outcomes. Further developing this modeling approach so that it can be applied in the clinical setting may help policy makers and physicians provide more accurate and detailed prognoses to patients and their families. Independent validation with more detailed therapeutic information from much larger cohorts, optimally from multiple medical centers, will be required before clinical implementation.

Comparison to Existing Methods for Predicting Post-Stroke Outcomes

Quantitative neuroimaging, especially in the context of the connectome, has become prevalent in recent studies aiming to link imaging biomarkers to impairments and recovery of function in stroke [Grefkes and Fink, 2014; Silasi and Murphy, 2014]. In stroke, the connectome plays an essential role in both continuing degeneration via diaschisis, i.e., the indirect disconnection/degeneration of remote areas due to spreading of the initial injury [Kuceyeski et al., 2014; Von Monakow, 1914; Puig et al., 2010], and recovery via modification/rewiring of damaged connections [Carter et al., 2012; Urbin et al., 2014]. Studies investigating changes to the functional connectome have been most prevalent [Carter et al., 2009; Ovadia-Caro et al., 2014], and are especially important in the context of non-invasive stimulation therapies like transcranial magnetic stimulation [Nouri and Cramer, 2011; Plow et al.,

2014]. Other approaches focus on the structural white matter connectome measured via diffusion MRI. These approaches include voxel- or region-based analysis of diffusion MRI metrics like fractional anisotropy (FA) [van Hees et al., 2014; Puig et al., 2013] and tractography, i.e., tracing of white matter connections [Burke Quinlan et al., 2015; Crofts et al., 2011; Johansen-Berg et al., 2010].

Most studies of long-term post-stroke outcome have focused on motor and language recovery. Puig et al., (2013) showed that the ratio of FA in the contra- versus ipsi-lesional cortico-spinal tract (CST) at 30 days was correlated with motor outcomes at 2 years. Another study found that combining diffusion MRI measures of the CST and gray matter volumetrics of the subcortical regions, in particular the caudate, best predicted long-term motor outcomes ($R^2 = 0.40$) [Yang et al., 2015]. In a study most similar to ours, Hope et al., (2013) predicted various long-term language outcomes with models based on demographic information and the stroke lesion's overlap with an atlas of white matter and gray matter ROIs ($R^2 = 0.34$–0.84). Despite the many studies in predicting long-term motor and language outcomes, there have been few studies analyzing the relationship between imaging biomarkers of the connectome measures of functions that influence overall cognitive and physical activities that determine an individual's daily quality of life, apart from specific motor or language abilities. One of the few studies we did find identified significant correlations between baseline FA in the CST with 1-month Barthel Index ($r = 0.72$, $R^2 = 0.51$) and Functional Independence Measure ($r = 0.71$, $R^2 = 0.50$) [Imura et al., 2015]. In another study, voxel-based lesion-symptom mapping was performed to identify areas that were important in post-stroke recovery of general ability [Cheng et al., 2014]. While that approach does not explicitly consider connectome disruption or allow prediction of a particular individual's outcome, it was one of the few to link imaging biomarkers to general recovery after stroke. The work presented in this paper appears to be one of the first to analyze the predictive power of different levels of structural connectome disruption on long-term post-stroke outcomes in various functional domains including cognition, motor and daily activities. In addition, the accuracy of our models ($R^2 = 0.56$-0.75) compares favorably to other models of post-stroke outcomes in general.

Despite their obvious utility, fMRI and tractography studies can be difficult to implement in the clinical setting. Both approaches require advanced post-processing expertise and additional resources for the acquisition of high quality non-clinical imaging in patient populations. An additional drawback specific to tractography in stroke patients is that pathological changes to brain tissue, particularly proximal to the lesion, may introduce noise into the diffusion MRI signal that can interfere with tractography results (see discussion in Crofts et al., 2011). The NeMo Tool circumvents these issues by using normal tractography data and lesion information to estimate resulting connectome disruptions and therefore may have greater potential to be clinically applied. Recently, a similar tool using normal functional connectome information was used to show associations between lesion location/size with symptom-relevant functional networks [Boes et al., 2015]. Tools based on normal connectome information that only require clinically acquired imaging to estimate connectome disruption should be made publicly available, enabling regular use by researchers and clinicians. It will result in improved consistency of biomarkers utilized in stroke studies, a wide-spread problem that has recently received attention [Harston et al., 2015].

Comparison of Models Based on the Varying Levels of Connectome Disruption

Models based on lesion volume and global network disruption performed similarly and had the worst accuracy for each outcome measure. None of the models had lesion volume or global imaging metrics as significant input variables. Lesion volume is highly correlated with global network metrics calculated using the NeMo Tool, which is why their models are essentially the same. Older patients tended to fare worse at their six-month follow-up in basic mobility, while females tended to do worse in both basic mobility and daily activity. This reflects many other studies finding that females tend to have poorer outcomes after stroke, particularly in physical or mobility activities [Fukuda et al., 2009; Patel et al., 2007; Petrea et al., 2009; Reeves et al., 2008; Roth et al., 2011]. Not surprisingly, discharge scores for two of the three metrics (Applied Cognitive and Basic Mobility) were significant predictors of six-month outcome scores. The months of rehabilitation variable was also a significant predictor in two of the three models. This was probably because patients with more severe functional limitations were likely to have more rehabilitation.

The fact that the lesion volume and global level models, arguably most similar to what is used clinically, performed the most poorly emphasizes the need for more detailed and quantitative measures of connectome disruption when developing prognoses for specific post-stroke functions. However, more anatomically specific disconnection measures are not always better, as can be seen from the comparison of the regional and pairwise level models. In fact, for two of the outcome measures, i.e., applied cognitive and basic mobility, the model based on disconnection measures at the level of gray matter regions had the best accuracy and minimum AIC. The model based on disconnection measures at the level of gray matter region pairs best predicted the subscore of daily living. We believe that the superior statistics in the regional level model for two of the outcome measures are a consequence of the care taken in this work to prevent overfitting (see Supporting Information Text I). Overfitting can occur when there are many more input variables than observations, a problem

that plagues the pairwise model to a greater extent than the regional model. Taken together, these results demonstrate that the accuracy of the model greatly depends on the level of detail of the input variables and, importantly, that it does not always increase with finer level of anatomical detail and concomitant increases in data dimensionality.

Relationships Between Disconnection Measures and Recovery

The regional-level models and the pairwise level models often had similarities between the areas that were significant predictors of each AMPAC subscore. By comparing Figures 5 and 6 we can see substantial overlap of the red and blue (both bright and pale) areas between the two figures.

Predicting recovery of applied cognitive measures

This outcome measure had the lowest accuracy and had the least localized coefficient values (over the brain) in both the regional and pairwise models compared to the models predicting the other two outcome measures. This is most likely due to the distributed nature of the brain networks involved in the tasks related to the Applied Cognitive measure, i.e., reading, writing, memory and comprehension. In fact, many regions important in both regional level and pairwise models are linked to these functions. Disconnection in many regions involved with controlling, planning, and sensing right body movement, i.e., the left pre/post/para central and middle frontal gyrus were important in the regional level model, which most likely influences writing and other right-dominant motor functions in these mostly right-handed subjects. In fact, the left superior and inferior parietal regions which are known to be central to writing in right-handed individuals [Menon and Desmond, 2001] were also significant predictors of the applied cognitive score in the regional level model. The right amygdala has been linked to declarative and episodic memory [McDonald and White, 1993], while lesions in the right cerebellum have been linked to verbal working memory deficits[Hokkanen et al., 2006]. Some right temporal and frontal regions, which overlap the right ventral attention network [Corbetta and Shulman, 2002], were also significant predictors of applied cognitive scores.

The remaining areas in the regional level model that were significant predictors were also significant in the pairwise model. These included the left dorsal striatum (caudate nucleus and putamen) and globus pallidus, which have been implicated in many higher-order executive functions like cognition involving motor function, decision making, stimulus-response learning [Balleine et al., 2007] and memory [McDonald and White, 1993]. The left superior frontal gyrus, which has been shown to be particularly important in working memory and spatially oriented processing [du Boisgueheneuc et al., 2006] was also important to both model levels.

Disconnection in a few regions, mostly in the left (non-motor) fronto-temporal areas and right motor areas, was associated with better outcomes in both the regional and pairwise level models. We speculate that this effect is due to the fact that if a person had a stroke in those areas then their left motor control/writing and right attention network areas that have large influences on the tasks measured with the Applied Cognitive score were most likely spared, allowing more complete recovery in this domain.

Predicting recovery of basic mobility measures

Four non-imaging input variables were important in predicting Basic Mobility in all model levels: age, gender, months of rehabilitation and discharge score. In addition, the left precentral and left middle frontal gyrus were especially important in both the regional and pairwise models (more disconnection = worse outcome). This is not surprising as the left precentral gyrus (primary motor area) is especially important for activities that fall within this category in our mostly right-handed subjects. The middle frontal gyrus has many executive, sensory processing and working memory functions [Fuster, 2008]. It also contains the dorso-lateral prefrontal cortex, which is known to be important in motor planning [Ferreira et al., 1998; Pochon, 2001]. In addition, the right anterior cingulate, which has been linked to various functions such as motivation [Holroyd and Yeung, 2012] and attention, particularly to behaviorally relevant stimuli [Weissman et al., 2005], was found to be important in predicting basic mobility in the pairwise model (more disconnection = worse outcome).

Predicting recovery of daily activity measures

In the regional model, disconnection in the right superior parietal gyrus was found to be a significant predictor of worse outcomes. The superior parietal regions are classically associated with visuo-spatial and attentional processing [Corbetta et al., 1995; Coull and Frith, 1998; Critchley, 1952]. Right superior parietal regions in particular have been shown by recent neuroimaging studies to be important in the manipulation of information in visual working memory [Berryhill and Olson, 2008; Koenigs et al., 2009]. Most interestingly, theoretical modeling work by Honey and Sporns (2008) suggested that lesions in the superior parietal area (Broadmann's areas 5 and 7) had the greatest potential to disrupt integrative aspects of neocortical function. The right middle frontal gyrus and right calcarine had significant positive coefficients indicating more disconnection was significantly associated with better outcomes. However, this was a weak association—the magnitude of the coefficient was about 10x smaller than the magnitude of that in the right superior parietal gyrus. The right middle frontal region, associated with left body movement among other functions, was also associated

with better Applied Cognitive measures. This indicated that stroke lesions in this area might relate to better long-term post-stroke recovery in different domains.

Significant coefficients in the pairwise-level model were mainly in right temporal-parietal regions, including right precuneus, rolandic operculum and angular gyrus, possibly implicating the ventral attention network's role in activities of daily living [Corbetta and Shulman, 2002]. Middle cingulate as well as the left middle frontal and bilateral motor areas also had significant negative coefficients, indicating adverse affects on the daily activity measure.

Limitations

There are potential sources of error in the data acquisition, image processing and model fitting. Because this work was based on clinically acquired imaging, there are some variations as to what scans were collected/available. In particular, about half of the subjects had T1 images and half the subjects had T2 images for coregistration of the lesion into the space of the NeMo Tool. However, T1- versus T2-based normalization effects were shown to be minimal in our previous NeMo Tool study with similar patients [Kuceyeski et al., 2014]. There are also potential sources of error in the lesion masking process. The manual approach used here was shown to have good Dice's inter-rater coefficient (0.77 ± 0.13), similar to our previous work [Kuceyeski et al., 2014]. T2 shine through, partial volume effects and other possible artifacts often must be dealt with by manual checking even if an automated algorithm is used to perform the initial masking. Therefore, there is some justification for the purely manual approach used here. Furthermore, we showed that the ChaCo and pairwise disconnection scores based on the different rater's masks had high correlation ($r = 0.97$ and 0.95, respectively). We conclude that the noise introduced at the level of the lesion masks has minimal impact on the final disconnection scores.

Another limitation is that the NeMo Tool uses a population of normal controls that are younger than our current stroke cohort. However, it must be emphasized that the NeMo Tool is not measuring connection, but disruptions of connection. For example, the regional disconnection (ChaCo) scores are measuring the percent of affected tracts out of the total connecting fibers. Even if there are fewer connections in an elderly normal population, the percent of affected tracts will be similar. Region-pair connections have the same justification—there we count the damaged fibers out of the total amount of fibers connecting two regions, which should be proportional between younger and older healthy controls. In addition, our previous lesion-dysfunction mapping study in a similar population (some patients were included in both studies) used the NeMo Tool to map disruptions of connectivity in eloquent regions to the proper associated patient dysfunction [Kuceyeski et al., 2015b]. Our previous work validating the NeMo Tool's application in this type of population increases confidence in the current results.

Finally, there are limitations related to the size of the data set and the noise present in the various measurements. While we are fairly confident that the results presented here provide insight into lesion-recovery relationships, the current study does lack proper model validation with independent test set of data. We did not explicitly reserve a portion of the data as a "test set" with which to validate the selected model created with the "training set" since we only had a moderate sample size. To compensate for this limitation, we chose to use strict statistical controls at every step in the model construction. We were very careful to cross-validate for the number of components in the PLSR models to avoid overfitting to the data. We also used bootstrapping to account for population makeup and strictly controlled for multiple comparisons when inspecting the regression coefficients' confidence intervals for the disconnection measures in the regional and pairwise models. Future studies using more subjects are planned in order to perform so-called nested validation, which will add further confidence in the extrapolation of the results to future observations. Other factors potentially important in predicting recovery may not have been included in the models, i.e., marital and living status, employment, other health issues etc. Finally, the AMPAC is based on self-assessment and therefore subject to the patient's interpretation. However, the majority of our discharge Applied Cognitive tests were independently performed by a therapist and there were very few cases of disagreement with the patient. In addition, a recent study showed that there was relatively good agreement between patient and proxy (family member or clinician) responses [Jette et al., 2012].

CONCLUSIONS

We successfully used structural connectome disruption information from the NeMo Tool to predict post-stroke recovery in different domains. Exploiting the ever-increasing knowledge of the human connectome, both structural and functional, will be critical if we are to understand impairment and recovery in stroke and other neurological disorders. Utilizing clinically acquired imaging and publicly available resources such as the NeMo Tool provides an effective way to increase the efficiency, power, reproducibility and generalizability of such studies. Focus must be directed to publicly available tools that can utilize clinically acquired imaging if we are to translate research findings into improved patient care. Ultimately, such tools could enable prediction of the effectiveness of different therapies for a particular individual after considering their particular pattern of connectome disruption. After more thorough validation with larger, more diverse datasets, these methods could be valuable quantitative tools for clinicians in developing prognoses and rehabilitation plans for post-stroke recovery.

REFERENCES

Andres PL, Black-Schaffer RM, Ni P, Haley SM (2004): Computer adaptive testing: A strategy for monitoring stroke rehabilitation across settings. Top Stroke Rehabil 11:33–39.

Auriat AM, Borich MR, Snow NJ, Wadden KP, Boyd LA (2015): Comparing a diffusion tensor and non-tensor approach to white matter fiber tractography in chronic stroke. NeuroImage Clin 7:771–781.

Balleine BW, Delgado MR, Hikosaka O (2007): The role of the dorsal striatum in reward and decision-making. J Neurosci 27: 8161–8165.

Belmonte MK, Allen G, Beckel-Mitchener A, Boulanger LM, Carper RA, Webb SJ (2004): Autism and abnormal development of brain connectivity. J Neurosci 24:9228–9231.

Berryhill ME, Olson IR (2008): The right parietal lobe is critical for visual working memory. Neuropsychologia 46:1767–1774.

Boes AD, Prasad S, Liu H, Liu Q, Pascual-Leone A, Caviness VS, Fox MD (2015): Network localization of neurological symptoms from focal brain lesions. Brain 228.

du Boisgueheneuc F, Levy R, Volle E, Seassau M, Duffau H, Kinkingnehun S, Samson Y, Zhang S, Dubois B (2006): Functions of the left superior frontal gyrus in humans: A lesion study. Brain 129:3315–3328.

Burke Quinlan E, Dodakian L, See J, McKenzie A, Le V, Wojnowicz M, Shahbaba B, Cramer SC (2015): Neural function, injury, and stroke subtype predict treatment gains after stroke. Ann Neurol 77:132–145.

Burnham K, Anderson D (2002): Model Selection and Multimodal Inference, 2nd ed. New York, NY: Springer-Verlag.

Carter AR, Astafiev SV, Lang CE, Connor LT, Rengachary J, Strube MJ, Pope DLW, Shulman GL, Corbetta M (2009): Resting state inter-hemispheric fMRI connectivity predicts performance after stroke. Ann Neurol 67:NA–NA.

Carter AR, Shulman GL, Corbetta M (2012): Why use a connectivity-based approach to study stroke and recovery of function? Neuroimage 62:2271–2280.

Cheng B, Forkert ND, Zavaglia M, Hilgetag CC, Golsari A, Siemonsen S, Fiehler J, Pedraza S, Puig J, Cho T-H, Alawneh J, Baron J-C, Ostergaard L, Gerloff C, Thomalla G (2014): Influence of stroke infarct location on functional outcome measured by the modified Rankin scale. Stroke 45:1695–1702.

Corbetta M, Shulman GL (2002): Control of goal-directed and stimulus-driven attention in the brain. Nat Rev Neurosci 3: 201–215.

Corbetta M, Shulman GL, Miezin FM, Petersen SE (1995): Superior parietal cortex activation during spatial attention shifts and visual feature conjunction. Science 80:802–805.

Coull JT, Frith CD (1998): Differential activation of right superior parietal cortex and intraparietal sulcus by spatial and nonspatial attention. Neuroimage 8:176–187.

Critchley M (1952): The Parietal Lobes. New York: Hafner.

Crofts J, Higham D, Bosnell R, Jbabdi S, Matthews PM, Behrens TEJ, Johansen-Berg H (2011): Network analysis detects changes in the contralesional hemisphere following stroke. Neuroimage 54:161–169.

Dice LR (1945): Measures of the amount of ecological association between species. Ecology 297–302.

Efron B (1987): Better bootstrap confidence intervals. J Am Stat Assoc 82:171–185.

Ferreira CT, Vérin M, Pillon B, Levy R, Dubois B, Agid Y (1998): Spatio-temporal working memory and frontal lesions in man. Cortex 34:83–98.

Friston KJ, Ashburner JT, Kiebel SJ, Nichols TE, Penny WD (2006): Statistical Parametric Mapping: The Analysis of Functional Brain Images. Academic Press, Cambridge, MA, USA.

Fukuda M, Kanda T, Kamide N, Akutsu T, Sakai F (2009): Gender differences in long-term functional outcome after first-ever ischemic stroke. Intern Med 48:967–973.

Fuster J (2008): The Prefrontal Cortex, 4th ed. Academic Press, Cambridge, MA, USA.

Glodzik L, Kuceyeski A, Rusinek H, Tsui W, Mosconi L, Li Y, Osorio RS, Williams S, Randall C, Spector N, McHugh P, Murray J, Pirraglia E, Vallabhajolusa S, Raj A, de Leon MJ (2014): Reduced glucose uptake and Aβ in brain regions with hyperintensities in connected white matter. Neuroimage

Grefkes C, Fink GR (2014): Connectivity-based approaches in stroke and recovery of function. Lancet Neurol 13:206–216.

Haley SM, Andres PL, Coster WJ, Kosinski M, Ni P, Jette AM (2004): Short-form activity measure for post-acute care. Arch Phys Med Rehabil 85:649–660.

Harston GWJ, Rane N, Shaya G, Thandeswaran S, Cellerini M, Sheerin F, Kennedy J (2015): Imaging biomarkers in acute ischemic stroke trials: A systematic review. Am J Neuroradiol 36:839–843.

van Hees S, McMahon K, Angwin A, de Zubicaray G, Read S, Copland DA (2014): Changes in white matter connectivity following therapy for anomia post stroke. Neurorehabil Neural Repair 28:325–334.

Hess CP, Mukherjee P, Han ET, Xu D, Vigneron DB (2006): Q-ball reconstruction of multimodal fiber orientations using the spherical harmonic basis. Magn Reson Med 56:104–117.

Hokkanen LSK, Kauranen V, Roine RO, Salonen O, Kotila M (2006): Subtle cognitive deficits after cerebellar infarcts. Eur J Neurol 13:161–170.

Holroyd CB, Yeung N (2012): Motivation of extended behaviors by anterior cingulate cortex. Trends Cogn Sci 16:122–128.

Honey CJ, Sporns O (2008): Dynamical consequences of lesions in cortical networks. Hum Brain Mapp 29:802–809.

Hope TMH, Seghier ML, Leff AP, Price CJ (2013): Predicting outcome and recovery after stroke with lesions extracted from MRI images. NeuroImage Clin 2:424–433.

Imura T, Nagasawa Y, Inagawa T, Imada N, Izumi H, Emoto K, Tani I, Yamasaki H, Ota Y, Oki S, Maeda T, Araki O (2015): Prediction of motor outcomes and activities of daily living function using diffusion tensor tractography in acute hemiparetic stroke patients. J Phys Ther Sci 27:1383–1386.

Iturria-Medina Y, Canales-Rodriguez E, Melie-Garcia L, Valdes-Hernandez P (2005): Bayesian formulation for fiber tracking. In:. Presented at the 11th Annual Meeting of the Organization for Human Brain Mapping. Toronto, Canada: NeuroImage. p 26.

Jette AM, Haley SM, Tao W, Ni P, Moed R, Meyers D, Zurek M (2007): Prospective evaluation of the AM-PAC-CAT in outpatient rehabilitation settings. Phys Ther 87:385–398.

Jette AM, Ni P, Rasch EK, Appelman J, Sandel ME, Terdiman J, Chan L (2012): Evaluation of patient and proxy responses on the activity measure for postacute care. Stroke 43: 824–829.

Johansen-Berg H, Scholz J, Stagg CJ (2010): Relevance of structural brain connectivity to learning and recovery from stroke. Front Syst Neurosci 4:146.

Koenigs M, Barbey AK, Postle BR, Grafman J (2009): Superior parietal cortex is critical for the manipulation of information in working memory. J Neurosci 29:14980–14986.

Krishnan A, Williams LJ, McIntosh AR, Abdi H (2011): Partial Least Squares (PLS) methods for neuroimaging: A tutorial and review. Neuroimage 56:455–475.

Kuceyeski A, Maruta J, Relkin N, Raj A (2013): The Network Modification (NeMo) Tool: Elucidating the effect of white matter integrity changes on cortical and subcortical structural connectivity. Brain Connect 3:451–463.

Kuceyeski A, Kamel H, Navi BB, Raj A, Iadecola C (2014): Predicting future brain tissue loss from white matter connectivity disruption in ischemic stroke. Stroke 45:717–722.

Kuceyeski A, Dayan M, Vargas W, Monohan E, Blackwell C, Raj A, Fujimoto K, Gauthier S (2015a): Modeling the relationship between gray matter atrophy, abnormalities in connecting white matter and cognitive performance in early Multiple Sclerosis. Am J Neuroradiol 36:702–709.

Kuceyeski A, Navi BB, Kamel H, Relkin N, Villanueva M, Raj A, Toglia J, O'Dell M, Iadecola C (2015b): Exploring the brain's structural connectome: A quantitative stroke lesion-dysfunction mapping study. Hum Brain Mapp 36:2147–2160.

Li Y, Liu Y, Li J, Qin W, Li K, Yu C, Jiang T (2009): Brain anatomical network and intelligence. PLoS Comput Biol 5:e1000395.

LoCastro E, Kuceyeski A, Raj A (2014): Brainography: An atlas-independent surface and network rendering tool for neural connectivity visualization. Neuroinformatics 12:355–359.

McDonald RJ, White NM (1993): A triple dissociation of memory systems: Hippocampus, amygdala, and dorsal striatum. Behav Neurosci 107:3–22.

McHugh ML (2012): Interrater reliability: The kappa statistic. Biochem medica 22:276–282.

Menon V, Desmond JE (2001): Left superior parietal cortex involvement in writing: Integrating fMRI with lesion evidence. Brain Res Cogn Brain Res 12:337–340.

Von Monakow C (1914): Die lokalisation im grosshirn und der abbau der funktion durch kortikale herde. J. F. Bergmann.

Mozaffarian D, Benjamin EJ, Go AS, Arnett DK, Blaha MJ, Cushman M, de Ferranti S, Després J-P, Fullerton HJ, Howard VJ, Huffman MD, Judd SE, Kissela BM, Lackland DT, Lichtman JH, Lisabeth LD, Liu S, Mackey RH, Matchar DB, McGuire DK, Mohler ER, Moy CS, Muntner P, Mussolino ME, Nasir K, Neumar RW, Nichol G, Palaniappan L, Pandey DK, Reeves MJ, Rodriguez CJ, Sorlie PD, Stein J, Towfighi A, Turan TN, Virani SS, Willey JZ, Woo D, Yeh RW, Turner MB (2014): Heart disease and stroke statistics-2015 update: A report from the American Heart Association. Circulation 131:e29–322.

Mukherjee P (2005): Diffusion tensor imaging and fiber tractography in acute stroke. Neuroimaging Clin N Am 15:655–665, xii.

Nouri S, Cramer SC (2011): Anatomy and physiology predict response to motor cortex stimulation after stroke. Neurology 77:1076–1083.

Ovadia-Caro S, Margulies DS, Villringer A (2014): The value of resting-state functional magnetic resonance imaging in stroke. Stroke 45:2818–2824.

Patel MD, McKevitt C, Lawrence E, Rudd AG, Wolfe CDA (2007): Clinical determinants of long-term quality of life after stroke. Age Ageing 36:316–322.

Petrea RE, Beiser AS, Seshadri S, Kelly-Hayes M, Kase CS, Wolf PA (2009): Gender differences in stroke incidence and post-stroke disability in the Framingham heart study. Stroke 40: 1032–1037.

Plow EB, Cunningham DA, Varnerin N, Machado A (2014): Rethinking stimulation of the brain in stroke rehabilitation: Why higher motor areas might be better alternatives for patients with greater impairments. Neuroscience 21:225–240.

Pochon J-B (2001): The role of dorsolateral prefrontal cortex in the preparation of forthcoming actions: An fMRI study. Cereb Cortex 11:260–266.

Puig J, Pedraza S, Blasco G, Daunis-I-Estadella J, Prats A, Prados F, Boada I, Castellanos M, Sánchez-González J, Remollo S, Laguillo G, Quiles AM, Gómez E, Serena J (2010): Wallerian degeneration in the corticospinal tract evaluated by diffusion tensor imaging correlates with motor deficit 30 days after middle cerebral artery ischemic stroke. AJNR Am J Neuroradiol 31:1324–1330.

Puig J, Blasco G, Daunis-I-Estadella J, Thomalla G, Castellanos M, Figueras J, Remollo S, van Eendenburg C, Sánchez-González J, Serena J, Pedraza S (2013): Decreased corticospinal tract fractional anisotropy predicts long-term motor outcome after stroke. Stroke 44:2016–2018.

Raj A, Kuceyeski A, Weiner M (2012): A network diffusion model of disease progression in dementia. Neuron 73:1204–1215.

Reeves MJ, Bushnell CD, Howard G, Gargano JW, Duncan PW, Lynch G, Khatiwoda A, Lisabeth L (2008): Sex differences in stroke: Epidemiology, clinical presentation, medical care, and outcomes. Lancet Neurol 7:915–926.

Roth DL, Haley WE, Clay OJ, Perkins M, Grant JS, Rhodes JD, Wadley VG, Kissela B, Howard G (2011): Race and gender differences in 1-year outcomes for community-dwelling stroke survivors with family caregivers. Stroke 42:626–631.

Seeley WW, Crawford RK, Zhou J, Miller BL, Greicius MD (2009): Neurodegenerative diseases target large-scale human brain networks. Neuron 62:42–52.

Seghier ML, Ramlackhansingh A, Crinion J, Leff AP, Price CJ (2008): Lesion identification using unified segmentation-normalisation models and fuzzy clustering. Neuroimage 41:1253–1266.

Šidák Z (1967): Rectangular confidence regions for the means of multivariate normal distributions. J Am Stat Assoc 62:626–633.

Siebens H, Andres PL, Pengsheng N, Coster WJ, Haley SM (2005): Measuring physical function in patients with complex medical and postsurgical conditions: A computer adaptive approach. Am J Phys Med Rehabil 84:741–748.

Silasi G, Murphy TH (2014): Stroke and the connectome: How connectivity guides therapeutic intervention. Neuron 83:1354–1368.

Skudlarski P, Jagannathan K, Anderson K, Stevens MC, Calhoun VD, Skudlarska BA, Pearlson G (2010): Brain connectivity is not only lower but different in schizophrenia: A combined anatomical and functional approach. Biol Psychiatry 68:61–69.

Smith SM, Jenkinson M, Woolrich MW, Beckmann CF, Behrens TEJ, Johansen-Berg H, Bannister PR, De Luca M, Drobnjak I, Flitney DE, Niazy RK, Saunders J, Vickers J, Zhang Y, De Stefano N, Brady JM, Matthews PM (2004): Advances in functional and structural MR image analysis and implementation as FSL. Neuroimage 23:S208–S219.

Sporns O, Tononi G, Kötter R (2005): The human connectome: A structural description of the human brain. PLoS Comput Biol 1:e42.

Stam CJ, Jones BF, Nolte G, Breakspear M, Scheltens P (2007): Small-world networks and functional connectivity in Alzheimer's disease. Cereb Cortex 17:92–99.

Supekar K, Menon V, Rubin D, Musen M, Greicius MD (2008): Network analysis of intrinsic functional brain connectivity in Alzheimer's disease. PLoS Comput Biol 4:e1000100.

Tzourio-Mazoyer N, Landeau B, Papathanassiou D, Crivello F, Etard O, Delcroix N, Mazoyer B, Joliot M (2002): Automated

anatomical labeling of activations in SPM using a macroscopic anatomical parcellation of the MNI MRI single-subject brain. Neuroimage 15:273–289.

Urbin MA, Hong X, Lang CE, Carter AR (2014): Resting-state functional connectivity and its association with multiple domains of upper-extremity function in chronic stroke. Neurorehabil Neural Repair 28:761–769.

Venkatasubramanian C, Kleinman JT, Fischbein NJ, Olivot J-M, Gean AD, Eyngorn I, Snider RW, Mlynash M, Wijman CAC (2013): Natural history and prognostic value of corticospinal tract wallerian degeneration in intracerebral hemorrhage. J Am Heart Assoc 2:e000090.

Warren DE, Power JD, Bruss J, Denburg NL, Waldron EJ, Sun H, Petersen SE, Tranel D (2014): Network measures predict neuropsychological outcome after brain injury. Proc Natl Acad Sci U S A 111:14247–14252.

Weissman DH, Gopalakrishnan A, Hazlett CJ, Woldorff MG (2005): Dorsal anterior cingulate cortex resolves conflict from distracting stimuli by boosting attention toward relevant events. Cereb Cortex 15:229–237.

Wen W, Zhu W, He Y, Kochan NA, Reppermund S, Slavin MJ, Brodaty H, Crawford J, Xia A, Sachdev P (2011): Discrete neuroanatomical networks are associated with specific cognitive abilities in old age. J Neurosci 31:1204–1212.

Yang M, Yang Y, Li H, Lu X, Shi Y, Liu B, Chen H, Teng G, Chen R, Herskovits EH (2015): Combining diffusion tensor imaging and gray matter volumetry to investigate motor functioning in chronic stroke. Ed. Annette Sterr. PLoS One 10:e0125038.

Zou KH, Warfield SK, Bharatha A, Tempany CMC, Kaus MR, Haker SJ, Wells WM, Jolesz FA, Kikinis R (2004): Statistical validation of image segmentation quality based on a spatial overlap index. Acad Radiol 11:178–189.